THE JOURNAL OF BIOLOGICAL CHEMISTRY
Vol. 273, No. 35, Issue of August 28, pp. 22627–22634, 1998
© 1998 by The American Society for Biochemistry and Molecular Biology, Inc.
*Printed in U.S.A.*

# A Heterotrimeric G Protein of the $G_i$ Family Is Required for cAMP-triggered Trafficking of Aquaporin 2 in Kidney Epithelial Cells*

(Received for publication, April 17, 1998, and in revised form, June 9, 1998)

**Giovanna Valenti‡, Giuseppe Procino‡, Ursula Liebenhoff§, Antonio Frigeri‡, Pio Alberto Benedetti¶, Gudrun Ahnert-Hilger‖, Bernd Nürnberg**, Maria Svelto‡, and Walter Rosenthal‡‡§§**

*From the ‡Dipartimento di Fisiologia Generale e Ambientale, Universitá degli Studi, 70126 Bari, Italy, §Rudolf-Buchheim-Institut für Pharmakologie, Justus-Liebig-Universität Gießen, 35392 Gießen, Germany, ‡‡Forschungsinstitut für Molekulare Pharmakologie, 10315 Berlin, Germany, ¶Istituto di Biofisica-CNR, 56127 Pisa, Italy, ‖Institut for Anatomie, Humboldt-Universität zu Berlin, 10115 Berlin, Germany, and **Institut für Pharmakologie, Freie Universität Berlin, 14195 Berlin, Germany*

**Vasopressin is the key regulator of water homeostasis in vertebrates. Central to its antidiuretic action in mammals is the redistribution of the water channel aquaporin 2 (AQP2) from intracellular vesicles to the apical membrane of kidney epithelial cells, an event initiated by an increase in cAMP and activation of protein kinase A. The subsequent steps of the signaling cascade are not known. To identify proteins involved in the AQP2 shuttle we exploited a recently developed cell line (CD8) derived from the rabbit cortical collecting duct and stably transfected with rat AQP2 cDNA. Treatment of CD8 cells with pertussis toxin (PTX) inhibited both the vasopressin-induced increase in water permeability and the redistribution of AQP2 from an intracellular compartment to the apical membrane. ADP-ribosylation studies revealed the presence of at least two major PTX substrates. Correspondingly, two $\alpha$ subunits of PTX-sensitive G proteins, $G\alpha_{i2}$ and $G\alpha_{i3}$, were identified by Western blotting. Introduction of a synthetic peptide corresponding to the C terminus of the $G_{i3}$ $\alpha$ subunit into permeabilized CD8 cells efficiently inhibited the cAMP-induced AQP2 translocation; a peptide corresponding to the $\alpha$ subunits of $G_{i1/2}$ was much less potent. Thus a member of the $G_i$ family, most likely $G_{i3}$, is involved in the cAMP-triggered targeting of AQP2-bearing vesicles to the apical membrane of kidney epithelial cells.**

Vasopressin is, by virtue of its antidiuretic action, the key regulator of water homeostasis in vertebrates. In mammals, the peptide hormone acts by redistributing the water channel AQP2[1] from intracellular vesicles to the apical membrane of kidney epithelial (principal) cells of the renal collecting duct (reviewed in Refs. 1 and 2). This event causes a rapid increase in the water permeability of the epithelial monolayer, thereby permitting reabsorption of water from the lumen of the collecting duct. As a consequence, urine osmolality increases and urinary output decreases.

In principal cells, vasopressin activates basolaterally located V2 receptors coupled to adenylyl cyclase by the cholera toxin-sensitive G protein $G_s$. The translocation of AQP2 is initiated by the hormone-induced rise in intracellular cAMP and the subsequent activation of cAMP-dependent protein kinase (3). The molecular events following this step, which eventually lead to the fusion of AQP2-bearing vesicles with the apical membrane, are not known.

GTP-binding proteins of remarkable diversity are key components in the regulation of vesicle movement between compartments of the exocytic and endocytic pathways (reviewed in Ref. 4). In particular, monomeric GTP-binding proteins of the Rab/YPT family have been assigned to various intracellular transport pathways (reviewed in Ref. 5). Rab3, a constituent of vesicles undergoing regulated excoytosis, has also been recently found in a kidney preparation enriched for AQP2-bearing vesicles (6); in further experiments the subtype has been determined as Rab 3a.[2] Heterotrimeric G proteins, traditionally thought to be transducer molecules confined to the plasma membrane, are also present on intracellular vesicles, and an increasing number of studies suggest that they participate in various intracellular transport pathways (reviewed in Refs. 7 and 8). In secretory, *e.g.* insulin-secreting cells (reviewed in Ref. 9), PTX, by uncoupling G proteins of the $G_i/G_o$ family from activated receptors by ADP-ribosylation of their $\alpha$ subunits, inhibits regulated exocytosis independent of signaling events across the plasma membrane.

To identify proteins involved in the AQP2 shuttle we exploited a recently developed cell line (CD8) (10), established by stably transfecting the RC.SV3 rabbit cortical collecting duct cells (11) with cDNA encoding rat AQP2. CD8 cells respond to vasopressin or forskolin with a 4–6-fold increase in the osmotic water permeability coefficient, $P_f$, and redistribution of AQP2 from an intracellular compartment to the apical membrane. Thus CD8 represent a unique model system, possessing the functional key properties of principal cells *in situ*. Here we show that a G protein of the $G_i$ family is required for cAMP-triggered trafficking of AQP2.

## EXPERIMENTAL PROCEDURES

*Culture and PTX Treatment of CD8 Cells*—CD8 cells (10) were established by stably transfecting the RC.SV3 rabbit cortical collecting duct cells (11) with cDNA encoding rat AQP2. CD8 cells were grown at 37 °C as described in a hormonally defined medium (10). Confluent monolayers were used at days 3–5 after plating. Cells grown on coverslips were incubated in the absence or presence of PTX (2 $\mu$g/ml, List Biological Laboratories) for 3 h at 37 °C and either stimulated with

* This work was supported by a grant from the Deutsche Forschungsgemeinschaft (Ro 597/6) and a grant from the Italian "Ministero Ricerca Scientifica e Tecnologica" (MURST, ex 40%). The costs of publication of this article were defrayed in part by the payment of page charges. This article must therefore be hereby marked "*advertisement*" in accordance with 18 U.S.C. Section 1734 solely to indicate this fact.

§§ To whom correspondence should be addressed. Tel.: 49-30-51551 218; Fax: 49-30-51551 291; E-mail: rosenthal@fmp-berlin.de.

[1] The abbreviations used are: AQP2, aquaporin 2; PTX, pertussis toxin; TIR, total internal reflection; $P_f$, osmotic water permeability coefficient; AS, antiserum; IC, intracellular; HSP, high speed pellet.

[2] U. Liebenhoff and W. Rosenthal, unpublished results.



Downloaded from http://www.jbc.org/ by guest on July 25, 2018

vasopressin or forskolin (15–20 min at 37 °C) or left under basal conditions. Thereafter, cells were prepared for TIR microfluorimetry or immunofluorescence microscopy.

*Osmotic Water Permeability Measurements by TIR Microfluorimetry*—The osmotically induced cell volume changes in adherent cells were measured by TIR microfluorimetry (13). Application of the procedure to CD8 cells and calculation of $P_f$ values have been described (10).

*Antibodies*—An affinity-purified antiserum (AS AQP2) raised against an AQP2 peptide has been characterized (10). A panel of rabbit antisera raised against synthetic peptides deduced from G protein subunits were employed: AS 8 raised against a peptide ((C)GAGESGKSTIVKQMK, G$\alpha_c$) common to various G protein $\alpha$ subunits including $G_s$, $G_i$, $G_o$, and $G_t$; AS 398 raised against a peptide ((C)TDDGMAVATGSWDDSFLKIWN, G$\beta_c$) common to G protein $\beta$ subunits (subtypes 1–4); AS 6 (affinity-purified) raised against a peptide ((C)NLKEDGISAAKDVK, G$\alpha_o$) specific for $G_o$ $\alpha$ subunits; AS 190 (affinity-purified) raised against a peptide (LDRIAQPNYI, G$\alpha_{i1}$) specific for the $G_{i1}$ $\alpha$ subunit; AS 373 raised against a peptide (DVIIKNNLKDCGLF, G$\alpha_{i1/2}$) specific for $G_{i1}$ and $G_{i2}$ $\alpha$ subunits; AS 269 raised against a peptide ((C)TGANKYDEAAS, G$\alpha_{i2}$) specific for the $G_{i2}$ $\alpha$ subunit; and AS 86 raised against a peptide (KNNLKECGLY, G$\alpha_{i3}$) specific for the $G_{i3}$ $\alpha$ subunits. An N-terminal C (in parentheses) in the sequence indicates an additional C used for coupling to keyhole limpet hemocyanin. Excepting antisera 190 and 373 the production of antisera and their specificity (as tested in Western blot and/or in immunoprecipitation experiments with recombinant G protein subunits) have been described (14, 15). In Western blot experiments AS 190 recognized specifically the $G_{i1}$ $\alpha$ subunit, and AS 373 recognized specifically $G_{i1}$ and $G_{i2}$ $\alpha$ subunits. The subunits recognized by the other antisera are mentioned under "Results."

*Conventional Immunofluorescence and Video Confocal Microscopy*—Conventional immunofluorescence and video confocal microscopy (16, 17) of CD8 cells grown on coverslips have been described (10). For video confocal microscopy, images were taken in the *xy* plane at steps of 320 nm, using an oil-immersion objective (40 × 1.40 normal aperture); *xz* sections were extracted from a set of planar images, the overall depth corresponding to about 6 $\mu$m.

*Effect of Peptides on cAMP-induced AQP2 Translocation and Quantitative Immunofluorescence*—CD8 cells grown on coverslips were washed three times in "intracellular" (IC) buffer (140 mM potassium glutamate, 20 mM Hepes, 5 mM $MgCl_2$, 5 mM EGTA, 5 mM NaCl, pH 7.4) at 37 °C. Permeabilization of cells was achieved using staphylococcal $\alpha$ toxin (18). The permeabilization was monitored by the cellular uptake of carboxyfluorescein (1.24 mM). Conditions in which more than 95% of cells were rendered fluorescent were selected. As an additional control for permeabilization, cAMP, which is membrane-impermeable, was used to elicit redistribution of AQP2 (see below). Cells were incubated for 10 min at 37 °C in the presence of $\alpha$ toxin in IC buffer devoid of peptides (control) or in IC buffer supplemented with peptides corresponding to the C termini of G protein $\alpha$ subunits (19). Thereafter, cells were washed three times in IC buffer and either incubated with 10 mM cAMP for 10 min at 37 °C or left under basal condition, fixed and immunostained with AS AQP2 (10). In addition to the G$\alpha_{i1/2}$ and G$\alpha_{i3}$ peptides (see above), a peptide (YLGLEKLNNK) with a reversed sequence with respect to the G$\alpha_{i3}$ peptide was employed. To quantify the effect of different peptides on cAMP-induced AQP2 redistribution in CD8 cells, AQP2 immunofluorescence intensity was analyzed in different experimental conditions. Briefly, planar images obtained by conventional immunofluorescence were analyzed using the Image Tool software which assigns to the brightest fluorescence detectable in the image a score of 255 and to the least fluorescence detectable a value of 1. All images had exactly the same pixel number in order to determine differences in the distribution of fluorescence between the different experimental groups. At least four randomly chosen boxes from different fields of the coverslips (corresponding to approximately 20 cells each) were analyzed from at least three separate experiments. Background fluorescence was measured and normalized. Images were processed, and the distribution of pixel intensity as a function of their frequency was determined for each image and relative parameters as standard deviation, skewness, and kurtosis were determined. Skewness is a measure of the symmetry of a profile about the mean pixel intensity value. Kurtosis describes the randomness of the shape of the profile relative to that of a perfectly random pixel intensity distribution. Statistical analyses were performed using the unpaired *t* test.

*Preparation of Cell Homogenates and Membranes*—Homogenates were prepared as described previously (10). For the preparation of crude membranes, cell monolayers were trypsinized, washed twice with phosphate-buffered saline, and homogenized with a glass/Teflon homogenizer in ice-cold buffer H (300 mM mannitol, 12 mM Hepes/Tris, pH 7.4). The suspension was centrifuged at 2,500 × *g* for 15 min, and the pellet containing nuclei and unbroken cells was discarded. The supernatant was spun at 10,000 × *g* for 10 min. The supernatant and the homogenized pellet were recombined, centrifuged at 100,000 *g* for 60 min, and the pellet was resuspended in phosphate-buffered saline, 0.1 mM phenylmethylsulfonyl fluoride. Crude membranes from rat kidney papilla or rabbit brain were prepared by cutting the tissues into small slices and homogenizing them in ice-cold buffer H. For the preparation of crude membranes, the resulting suspension was subjected to the protocol described above. For the preparation of high speed pellet (HSP) from rabbit kidney papilla, the papillae were excised and homogenized with a glass/Teflon homogenizer in ice-cold buffer H. The suspension was centrifuged at 700 × *g* for 10 min at 4 °C. The supernatant was centrifuged at 17,000 × *g* for 45 min at 4 °C. The supernatant was spun at 200,000 × *g* in a Beckman Rotor 60 Ti for 60 min at 4 °C. The final pellet (HSP) enriched in intracellular vesicles, was recovered in buffer H and used for immunoblot experiments.

*Preparation of AQP2-containing Vesicles ("Endosomes")*—Endosomes were prepared from rat kidney papillae or CD8 cells according to Sabolic *et al.* (20) with slight modifications. Briefly, the kidney papillae from six rats were excised and cut into small pieces. These pieces or CD8 cells from confluent monolayers grown in six 175-$cm^2$ culture flasks were homogenized with a glass/Teflon homogenizer in ice-cold buffer H. The suspension was centrifuged at 2,500 × *g* at 4 °C, and the supernatant was recentrifuged at 20,000 × *g* for 20 min at 4 °C. The obtained supernatant and the upper part of the pellet were centrifuged at 45,000 × *g* for 60 min at 4 °C. The pellet was recovered, resuspended in 1.5 ml of buffer H, homogenized with a manual glass Potter, loaded on an 18% Percoll gradient and centrifuged at 45,000 × *g* for 50 min at 4 °C. The opalescent part of the gradient located in the bottom third of the gradient was recovered, resuspended in KCl buffer (300 mM mannitol, 100 mM KCl, 5 mM $MgSO_4$, 15 mM Hepes/Tris, pH 7.0), and centrifuged at 45,000 × *g* for 60 min at 4 °C. The pellet containing AQP2-enriched vesicles was recovered in buffer H.

*[$^{32}$P]ADP-ribosylation of Proteins and Western Blotting*—PTX-catalyzed [$^{32}$P]ADP-ribosylation of proteins and analysis of radiolabeled proteins were carried out as described previously (15). Western blotting was performed as described elsewhere (10) except that proteins were separated by 10% SDS gels in the presence of 1 M urea. Filters were incubated with primary antibodies diluted as indicated and thereafter with alkaline phosphatase-conjugated goat anti-rabbit IgG (1:5000, Sigma). Immunoreactive proteins were visualized by a color reaction (10).

## RESULTS

*PTX Inhibits the Forskolin-induced Increase in Water Permeability and AQP2 Trafficking*—To test whether G proteins are involved in the AQP2 redistribution downstream of the cAMP/cAMP-dependent protein kinase signal, we treated CD8 cells with PTX which ADP-ribosylates and thereby uncouples G proteins of the $G_i$ and $G_o$ types from their cognate receptors. The time course of cell swelling in response to changes in perfusate osmolality was measured by TIR microfluorimetry (Fig. 1; see "Experimental Procedures"). In control cells, forskolin, a strong direct activator of adenylyl cyclase, accelerated cell swelling in response to a decrease in perfusate osmolality by 200 mM (Fig. 1*A*); it also increased the extent of swelling in the observed time interval (45 s). The change in fluorescence caused by forskolin corresponds to an about 5-fold increase in the $P_f$ (Fig. 1*C*). When cells had been treated with PTX, the time course of cell swelling (Fig. 1*B*) and water permeability (Fig. 1*C*) were not modified by forskolin. The data suggest that PTX either inhibits AQP2 trafficking or impairs AQP2 function.

To differentiate between these possibilities we examined the effect of PTX on the vasopressin-induced redistribution of AQP2 (Fig. 2). Control or PTX-treated CD8 cells grown on coverslips were fixed, immunostained with AS AQP2 (for Western blot analysis of CD8 cells with the same antiserum, see Fig. 7), and examined by video confocal microscopy (see "Experimental Procedures"). In control cells under resting conditions, both intracellular and apical plasma membrane staining was observed; stimulation of cells with vasopressin resulted in an increased staining to the apical membrane and an increase in cell height (Fig. 2, *upper panel*) (10). After treatment with PTX,

Downloaded from http://www.jbc.org/ by guest on July 25, 2018

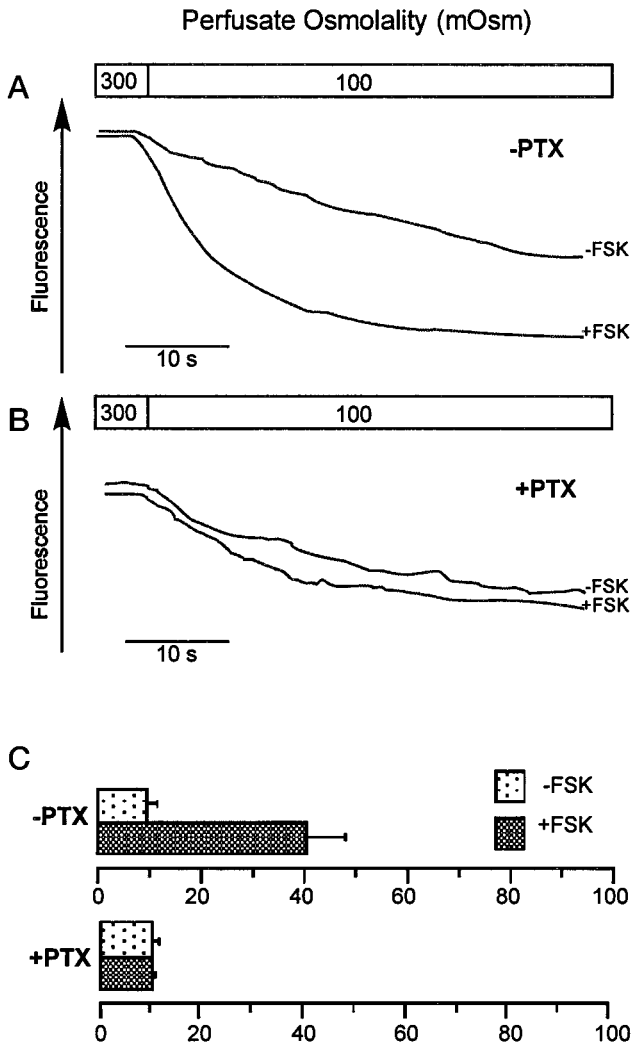


FIG. 1. *Panels A* and *B*, representative TIR fluorescence time courses of CD8 cells at 10 °C in response to a 200 mOsm inwardly directed NaCl gradient. In the absence of PTX (−*PTX*, *panel A*), forskolin (*FSK*; $10^{-4}$ M for 15 min) caused a dramatic increase in the rate of cell swelling. When cells were pretreated with PTX (+*PTX*, *panel B*) FSK had no effect on the rate of cell swelling. *Panel C*, mean values ± S.E. ($n = 3$) of $P_f$ [($\times 10^{-4}$) cm/s] calculated from TIR fluorescence time courses.

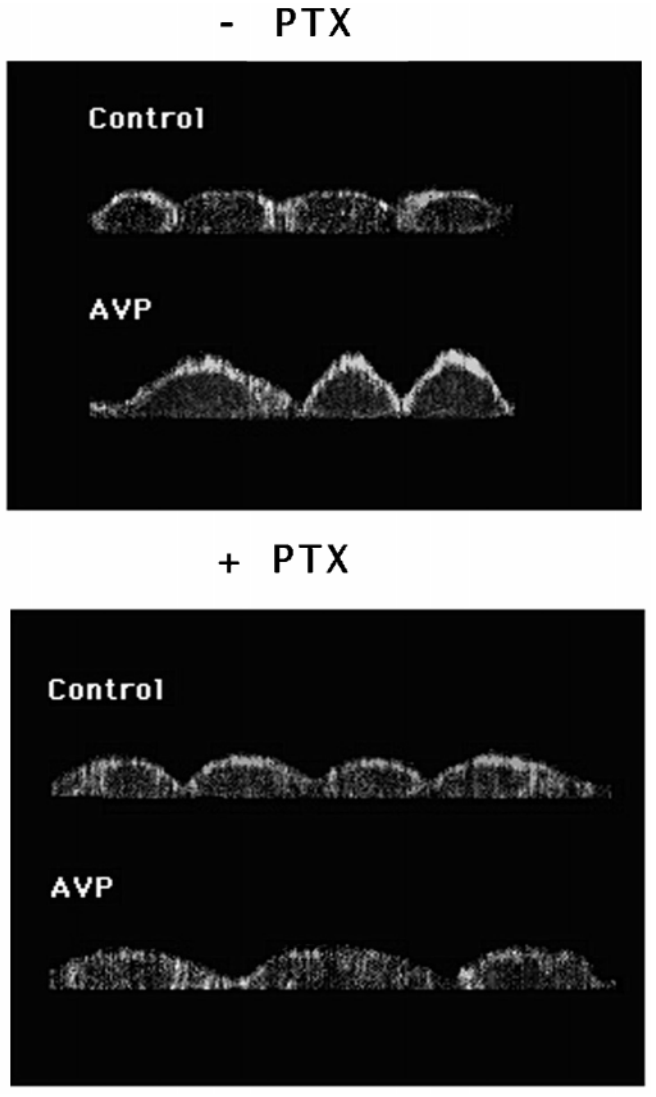


FIG. 2. **Video confocal microscopy of CD8 cells.** Cells grown on coverslips were incubated in the absence (−*PTX*) or presence of PTX (+*PTX*) and either stimulated with vasopressin (*AVP*; 10 nM for 20 min at 37 °C) or left under basal conditions (*Control*). The cells were fixed and immunostained with AS AQP2. Shown is an xz section calculated from a set of xy images (*bottom*, plane of coverslip).

vasopressin failed to induce a redistribution (Fig. 2, *lower panel*). Similar data were obtained when forskolin was used instead of vasopressin (not shown) (10). These findings fully explain the lack of a functional response in PTX-treated cells and show that a PTX substrate is required for the cAMP-induced redistribution of AQP2.

*Identity of the G Protein Involved in AQP2 Trafficking*—Further experiments were performed to identify the PTX substrates involved in AQP2 trafficking. Fractions from CD8 cells (total cell homogenate, crude membranes and a fraction enriched for AQP2-bearing vesicles traditionally termed endosomes; see "Experimental Procedures") were incubated with [$^{32}$P]NAD in the absence or presence of PTX, and [$^{32}$P]ADP-ribosylated proteins were analyzed by high resolution SDS-polyacrylamide gel electrophoresis followed by autoradiography (Fig. 3). In brain membranes, a rich source for PTX-sensitive G proteins of the $G_i$ and $G_o$ families, a strong signal was detected at 39–45 kDa. Among the various preparations of CD8 cells the strongest signal was observed in the endosome fraction. Whereas a weak signal was seen in the homogenate, apparently two major substrates were found in the 43-kDa region in the crude membrane and endosome preparations. As shown below, the PTX substrates in CD8 cells correspond to $\alpha$ subunits of the $G_i$ family. The relatively high apparent molecular masses of PTX substrates ($G_i/G_o$ $\alpha$ subunits) are due to the presence of 6 M urea during SDS-polyacrylamide gel electrophoresis (15).

To determine functionally the involvement of G proteins in the regulation of AQP2 trafficking, we permeabilized CD8 cells with $\alpha$ toxin as described previously (18). The holes formed by the toxin (2–3 nm in diameter) allow the introduction of small molecules such as peptides into the interior of cells. Control experiments were carried out to determine the appropriate concentration of the toxin which allowed the permeabilization without loss of cellular responsiveness to cAMP in terms of AQP2 redistribution (see "Experimental Procedures"). Permeabilized CD8 cells were exposed to peptides, stimulated with cAMP, fixed, immunostained with AS AQP2, and analyzed by video confocal microscopy (Fig. 4). The $G\alpha_{i1/2}$ and $G\alpha_{i3}$ peptides employed (see "Experimental Procedures") corresponded to the C-terminal domains of human $G_{i1/2}$ and $G_{i3}$ $\alpha$ subunits, respectively, and include the cysteine residue modified by PTX. Previous studies have shown that peptides corresponding to the C

Downloaded from http://www.jbc.org/ by guest on July 25, 2018

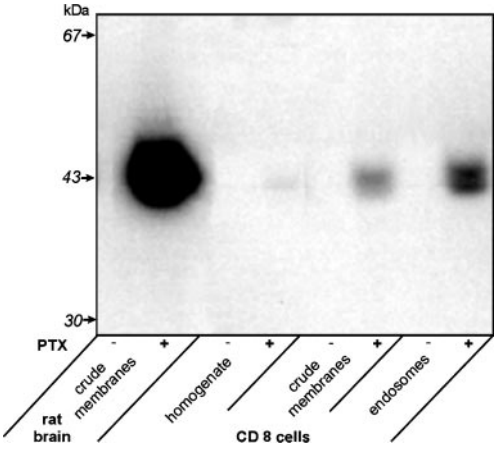


FIG. 3. **PTX substrates in CD8 cells.** The indicated fractions from rat brain and CD8 cells were incubated with [$^{32}$P]NAD in the absence (−) or (presence (+) of PTX. Proteins were separated by SDS-polyacrylamide gel electrophoresis in the presence of 6 M urea, and $^{32}$P-labeled proteins were visualized by autoradiography. The selected film shows substrates in all preparations (including a weak signal in CD8 cell homogenate).

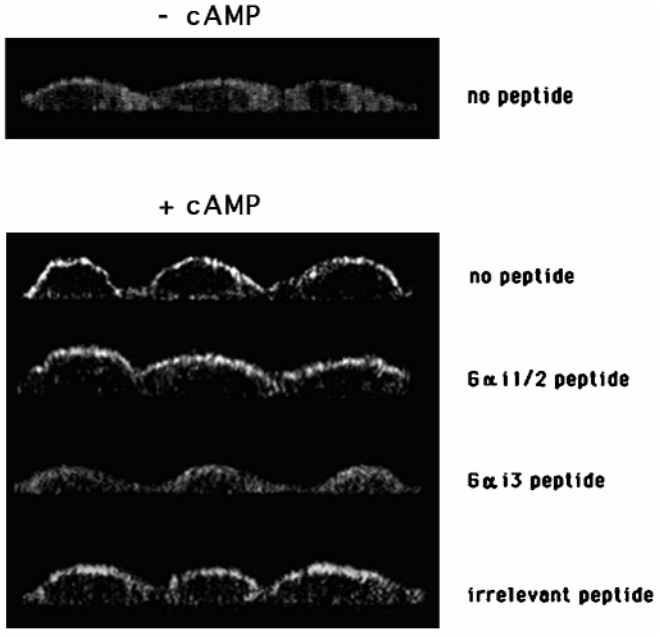


FIG. 4. **Effect of peptides on cAMP-induced AQP2 translocation in permeabilized CD8 cells.** Cells grown on coverslips were permeabilized with $\alpha$ toxin in the absence of peptides (no peptide) or in the presence of $G\alpha_{i1/2}$ peptide (100 $\mu$g/ml), $G\alpha_{i3}$ peptide (100 $\mu$g/ml), or a peptide (100 $\mu$g/ml) having a reversed sequence with respect to the $G\alpha_{i3}$ peptide (*irrelevant peptide*). Cells were then washed and incubated with 10 $\mu$M cAMP (+*cAMP*). Control experiments were performed with permeabilized cells left under basal conditions (−*cAMP*; *top panel*). The cells where fixed, stained with AS AQP2, and analyzed by video confocal microscopy (*xz* scans).

termini of $\alpha$ subunits inhibit coupling of G proteins to their cognate receptors (19).

In the basal state (Fig. 4; −*cAMP*), permeabilized CD8 cells showed a diffuse distribution of AQP2. After stimulation with cAMP a marked increase in apical staining was seen in cells incubated in the absence of peptides, in the presence of the $G\alpha_{i1/2}$ peptide (100 $\mu$g/ml), and in the presence of a peptide (100 $\mu$g/ml) with the composition of the $G\alpha_{i3}$ peptide but a reversed sequence. In contrast, diffuse intracellular staining, similar to that in nonstimulated cells, was observed in the presence of the $G\alpha_{i3}$ peptide (100 $\mu$g/ml). The data indicate that the $G\alpha_{i3}$ peptide inhibits the cAMP-induced redistribution of AQP2.

*Quantification of the Peptide Effect on cAMP-triggered AQP2 Translocation*—To quantify the effect of different peptides, we next applied image analysis methods based on AQP2 signal intensity in CD8 cells. Cells were stained with AS AQP2 under different experimental conditions, and planar images, obtained by conventional immunofluorescence microscopy, were analyzed using the Image Tool software that assigns to the brightest fluorescence detectable in the image a score of 255 and to the least fluorescence detectable a value of 1 (see "Experimental Procedures"). A representative experiment is shown in Fig. 5. Under basal conditions, a punctate intracellular AQP2 staining is visible. As previously shown (10), addition of vasopressin causes the disappearance of intracellular staining because of the redistribution of AQP2 in the apical membrane; forskolin has a similar effect (not shown). The relative pixel intensity plotted as a function of their frequency (*lower panels*) is substantially different under nonstimulated and stimulated conditions. Whereas a random pixel intensity distribution characterizes the basal condition, most of the pixels are in a narrow range of a low intensity gray scale under stimulated conditions.

Using these tools, we evaluated quantitatively the effects of each peptide at different concentrations on cAMP-induced AQP2 redistribution. To this end, quantitative image features, skewness and kurtosis, were derived from automated analysis of digitized planar images. The two parameters were calculated for at least three independent experiments. For each experiment, at least four images were obtained from different fields of the coverslips (see "Experimental Procedures"). In nonstimulated permeabilized cells kurtosis and skewness were 3.4 ± 0.3 and 2.1 ± 0.05 (mean values ± S.D.; $n = 4$), respectively. The coefficients obtained with cAMP-stimulated CD8 cells were 20.35 ± 1.05 (kurtosis) and 4.55 ± 0.09 (skewness). A representative experiment performed with cAMP-stimulated cells is shown in Fig. 6. The coefficient values for cells incubated with cAMP and the $G\alpha_{i1/2}$ peptide at concentrations up to 100 $\mu$g/ml did not significantly differ from those obtained for cAMP-stimulated cells receiving the same concentrations of the irrelevant peptide or no peptide. Only at a concentration of 200 $\mu$g/ml of the $G\alpha_{i1/2}$ peptide were the two coefficients significantly lowered ($p < 0.05$). In contrast, the $G\alpha_{i3}$ peptide highly significantly ($p < 0.0001$) decreased both coefficients in cAMP-stimulated cells at all concentrations tested (50, 100, and 200 $\mu$g/ml). Interestingly, the values for kurtosis and skewness in nonstimuated cells (see above) were nonsignificantly different from those obtained with cAMP-stimulated cells incubated with the $G\alpha_{i3}$ peptide at concentrations of 100 $\mu$g/ml (kurtosis, 3.7 ± 0.60; skewness, 2.2 ± 0.06) or 200 $\mu$g/ml (kurtosis, 3.2 ± 0.70; skewness, 2.2 ± 0.16). The data suggest a complete block of AQP2 translocation by the $G\alpha_{i3}$ peptide used at concentrations ≥100 $\mu$g/ml. For cells incubated with the $G\alpha_{i3}$ peptide at 50 $\mu$g/ml, kurtosis and skewness differed, however, significantly from those found for unstimulated cells ($p < 0.005$ and $p < 0.01$, respectively).

*G Protein Subunits in CD8 Cells*—As a next step, we analyzed the subcellular distribution of G protein subunits in CD8 cells by performing Western blot experiments with a panel of anti-peptide antibodies. In contrast to Fig. 3, SDS gels with 1 M urea were used to separate proteins prior to blotting (Fig. 7). In some panels, an immunoreactive band at ≥42 kDa is visible in the membrane preparation from rabbit kidney enriched in endosomes (HSP). Further analysis revealed that this signal was entirely due to an unspecific staining by a batch of secondary antibodies; it was not observed in the absence of primary antibodies.

AS AQP2 (*AQP2* in Fig. 7) was used to estimate AQP2 levels in the different preparations. As described elsewhere (10), the

Downloaded from http://www.jbc.org/ by guest on July 25, 2018

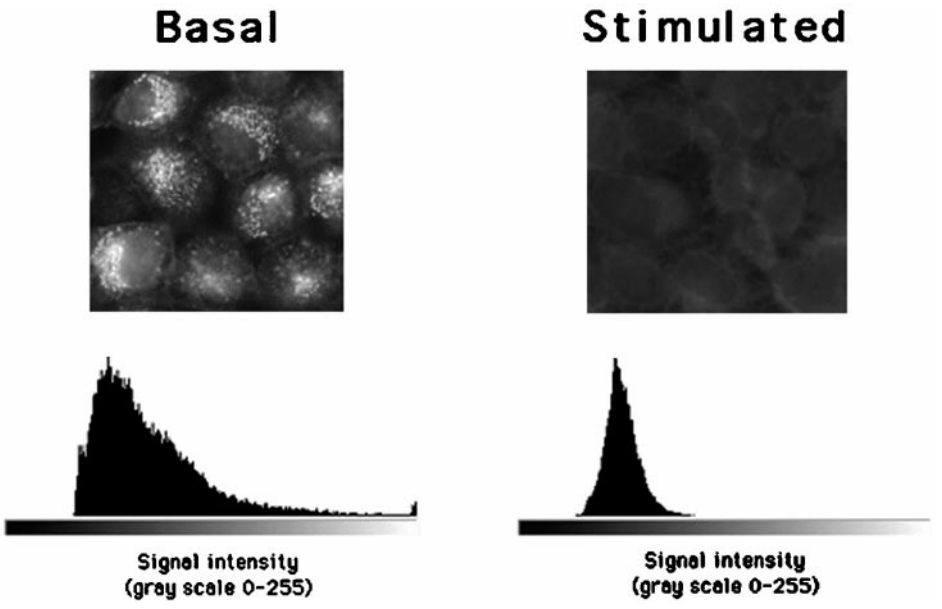


FIG. 5. **Representative distribution of relative pixel intensity as a function of their frequency in CD8 cells stained with AS AQP2 under basal condition and after stimulation with vasopressin (10 nM).** After hormonal stimulation, most of the pixels are concentrated in a narrow range of gray scale characterized by a low intensity, whereas a random pixel intensity distribution is typical for the basal condition.

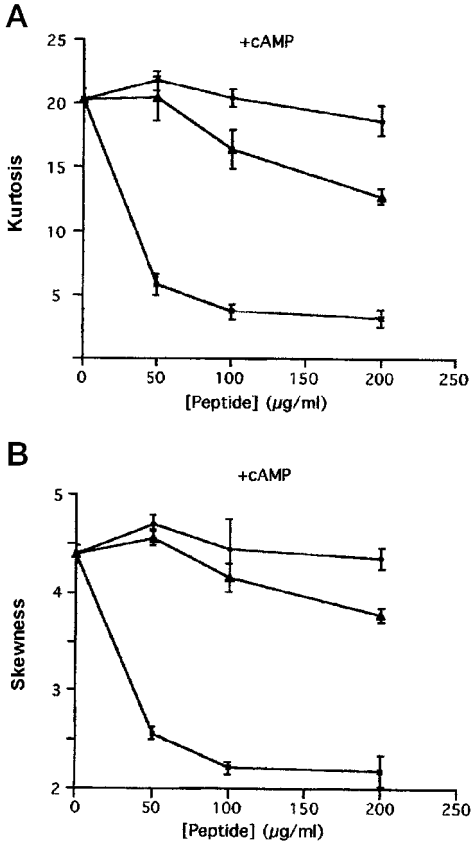


FIG. 6. **Quantification of the effects of peptides on cAMP-triggered AQP2 translocation by quantitative image analysis.** Cells were incubated with different concentrations of the $G\alpha_{i3}$ peptide (■), the G $\alpha_{i1/2}$ peptide (▲), or the irrelevant peptide (●) and stimulated with cAMP. Two parameters, kurtosis (*A*) and skewness (*B*), were calculated using Image Tool software (see "Experimental Procedures"). Each experimental point represents the mean ± S.D. of the parameters obtained from four images of a representative experiment. Similar results were obtained in at least three independent experiments.

antiserum detects the nonglycosylated and glycosylated forms of rat AQP2 at 29–30 and 35–45 kDa, respectively. The AQP2 signal was strongest in the endosome fractions either from CD8 cells, which overexpress rat AQP2, or from rat kidney. In a membrane preparation from rabbit kidney enriched in intracellular vesicles (HSP), the antibody stained a 29-kDa band (unglycosylated form of AQP2). A band corresponding to the glycosylated form of AQP2 was barely visible in the rabbit kidney. Since AS AQP2 was raised against a C-terminal peptide of AQP2 from rat, it is possible that it reacts poorly with the rabbit protein, although other reasons for the weak signal have not been excluded. AS 8 ($G\alpha_c$ in Fig. 7), which preferentially recognizes the $\alpha$ subunits of $G_i$ and $G_o$ (39–41 kDa), stained a band in the 40-kDa region in all preparations. The strong signal in rabbit brain membranes reflects the high level expression of $G_i/G_o$ $\alpha$ subunits. In CD8 cells, the 40-kDa signal was weak in the homogenate, stronger in the crude membrane preparation, and strongest in the endosomes preparation, consistent with the ADP-ribosylation data (Fig. 3). HSP from rabbit kidney and crude membranes from rat kidney also yielded prominent signals. An antiserum (AS 6; $G\alpha_o$) specific for $G_o$ $\alpha$ subunits detected a 39-kDa protein in rabbit brain membranes but not in CD8 cells or rabbit and rat kidney preparations, indicating that $G_o$ is not expressed in the kidney or CD8 cells. Thus the immunoreactive 40-kDa proteins in CD8 cells and rabbit kidney papilla/medulla represent $G_i$ $\alpha$ subunits.

The preferred substrates of PTX are $G_{i/o}$ $\alpha$ subunits associated with $\beta\gamma$ complexes; in contrast, monomeric $\alpha$ subunits are very poor substrates (see, *e.g.* Ref. 21). The strong signals obtained for endosomes of CD8 cells (Fig. 3) suggests that G proteins in this preparation are heterotrimers. Since $\beta$ subunits are always associated with $\gamma$ subunits under native conditions, the detection of $\beta$ subunits is equivalent to that of $\beta\gamma$ complexes. We therefore employed AS 398 ($G\beta_c$ in Fig. 5) which recognizes $\beta$ subunits (subtypes 1–4). The antibody stained a 35–36 kDa band in all preparations. Excepting the homogenate of CD8 cells, the relative intensity of the signals obtained with AS 398 is reminiscent to that obtained with AS 8, suggesting a similar distribution of $\alpha$ and $\beta$ subunits.

In view of the functional effects of PTX, we analyzed CD8 cells in greater detail for the presence of $G_i$ $\alpha$ subunits. AS 190 ($G\alpha_{i1}$ in Fig. 7), specific for $G_{i1}$ $\alpha$ subunits, easily detected a protein of the appropriate size (40 kDa) in rabbit brain membranes and in crude membranes from rat kidney, whereas no or very weak signals were obtained with CD8 cell preparations. A relatively weak signal was also found in rabbit kidney. Because of the strong signal observed in rabbit brain, the weak signal observed in CD8 cells cannot be explained by species specificity of AS 190. The data rather indicate that rabbit kidney and CD8

Downloaded from http://www.jbc.org/ by guest on July 25, 2018

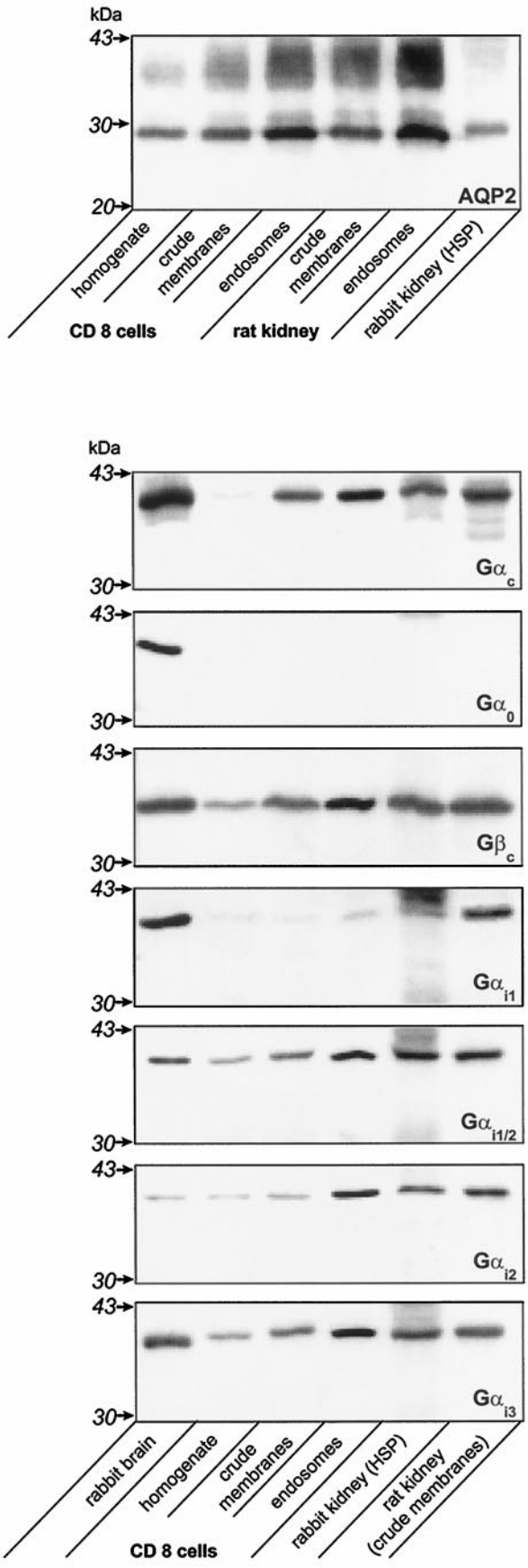


FIG. 7. **Detection of AQP2, G protein $\alpha$ and $\beta$ subunits in CD8 cells, rabbit and rat kidney papilla/medulla, and rabbit brain.** Onto each lane of an SDS gel, 60 $\mu$g of protein were loaded. Proteins were separated by SDS-polyacrylamide gel electrophoresis and transferred onto membranes, which were incubated with the primary antipeptide antisera indicated on the *bottom right* of each panel. The AQP2 antiserum and AS 190 ($G\alpha_{i1}$) were subjected to affinity chromatography prior to use. The dilutions of the other antisera were 1:5000. Immunoreactive proteins were visualized by a color reaction. Molecular masses are indicated on the left.

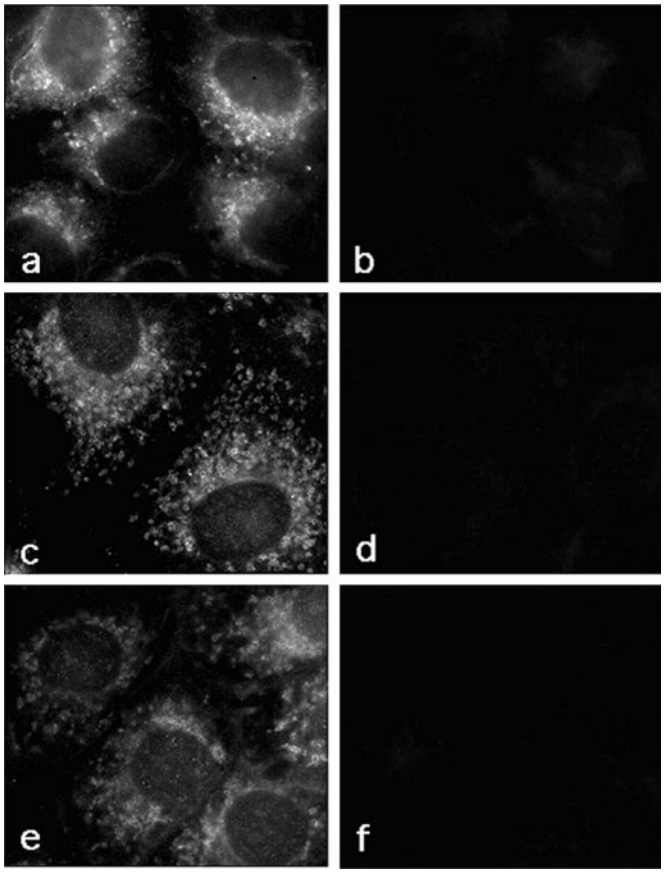


FIG. 8. **Localization of AQP2 and $G_i$ $\alpha$ subunits in CD8 cells.** Cells were analyzed by conventional immunofluorescence microscopy. The primary anti-peptide-antisera were: AS AQP2 (*a*), AS 86 (raised against the $G\alpha_{i3}$ peptide; *c*) and AS 373 (raised against the $G\alpha_{i1/2}$ peptide; *e*). Control experiments with peptide-adsorbed antibodies are shown on the corresponding *right panels*. Magnification, × 700.

cells derived thereof express $G_{i1}$ $\alpha$ subunits at low levels.

AS 373 ($G\alpha_{i1/2}$ in Fig. 7), raised against the $G\alpha_{i1/2}$ peptide employed in the functional studies (Fig. 4), readily detected a 40-kDa protein in all preparations. Since AS 373 recognizes both $G_{i1}$ and $G_{i2}$ $\alpha$ subunits, we further employed AS 269 ($G\alpha_{i2}$ in Fig. 7) raised against a central portion of the polypeptide chain forming the $G_{i2}$ $\alpha$ subunit; the antiserum recognizes only the $G_{i2}$ $\alpha$ subunit. AS 269 recognized a 40-kDa protein in all preparations. This finding also applies to AS 86 ($G\alpha_{i3}$ in Fig. 7) which was raised against the $G\alpha_{i3}$ peptide used in the experiments with permeabilized cells (Fig. 4) and reacts only with $G_{i3}$ $\alpha$ subunits. The signals obtained with the AS 393, AS 269, and AS 86 were stronger in CD8 cell endosomes than in the homogenates or the unfractionated membranes. The same antisera stained a prominent band in HSP from rabbit kidney and in rat kidney membranes. The data show that $G_{i2}$ and $G_{i3}$ $\alpha$ subunits are easily detectable in CD8 cell fractions, including a fraction enriched for AQP2-bearing vesicles.

To study further the subcellular distribution of G protein $\alpha$ subunits, we subjected nonstimulated CD8 cells to conventional immunofluoresence microscopy. The experiments were performed with AS 373 and AS 86 since the two antisera were specific for $G_i$ $\alpha$ subunits in Western blot experiments (Fig. 7) and the peptides used for generating them were employed in

Downloaded from http://www.jbc.org/ by guest on July 25, 2018

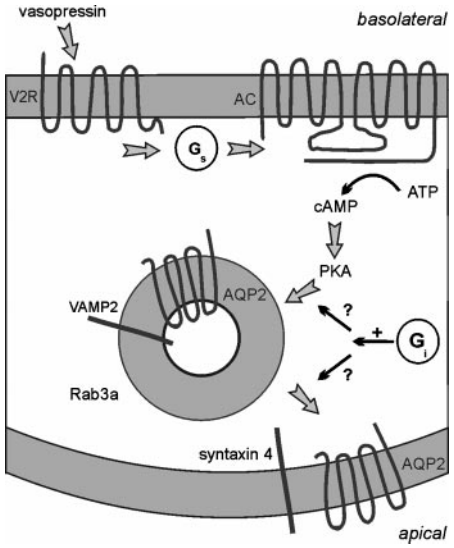


FIG. 9. **A cellular model for vasopressin/cAMP-induced AQP2-trafficking in renal collecting duct principal cells.** The mechanisms underlying docking and fusion of AQP2-bearing vesicles are not known. The detection of the small GTP-binding protein Rab3a (6) (U. Liebenhoff and W. Rosenthal, unpublished results), synaptobrevin 2, here referred to as *VAMP2* (6, 30, 32), and syntaxin 4 (31) in principal cells suggests that these proteins are involved in AQP2 trafficking. We show here that a G protein of the $G_i$ family is required for AQP2 trafficking downstream of the cAMP/cAMP-dependent protein kinase (*PKA*) signal. Its precise role remains to be determined (see "Discussion").

functional studies (Fig. 4); AS AQP2 was used as a control. The staining pattern obtained with AS AQP2 (Fig. 8*a*) is consistent with an intracellular location of AQP2 (10). Strong intracellular staining was also observed with AS 86 (Fig. 8*c*) and AS 373 (Fig. 8*e*). The signals were completely suppressed by preincubation of the antisera with the respective peptide used for immunization (Fig. 8, *b*, *d*, and *f*). Surprisingly, the images suggest a predominantly intracellular location of $G_i$ $\alpha$ subunits. Typically, a punctate staining was observed in the perinuclear region, along with extensions to the cell surface. The data do not exclude the presence of $G_i$ $\alpha$ subunits on the plasma membrane; however, their abundance at this location must be low compared with that at intracellular sites. Although the structures bearing $G_i$ $\alpha$ subunits remain to be characterized, the present data are consistent with the view that they include but are not limited to the Golgi complex. In agreement with the Western blot data (Fig. 7), AS 190, which specifically recognizes the $G_{i1}$ $\alpha$ subunit, failed to stain CD8 cells (not shown). Other authors have shown that $G_{i3}$ $\alpha$ subunits are present on the Golgi membranes of a proximal kidney tubule cell line, LLC-PK1 (22).

## DISCUSSION

Vasopressin exerts its antidiuretic effect by translocating AQP2 from intracellular compartments to the apical plasma membrane of renal collecting duct principal cells. The primary cellular targets of vasopressin are V2 receptors coupled to adenylyl cyclase *via* the cholera toxin-sensitive G protein $G_s$. Activation of this pathway leads to an increase in intracellular cAMP levels and activation of cAMP-dependent protein kinase. It has been suggested that phosphorylation of AQP2 by cAMP-dependent protein kinase plays a role in hormonally induced AQP2 trafficking (23, 24). Here we show that a second G protein is essential for the vasopressin-induced shuttle of AQP2. This G protein is sensitive to PTX and is involved in the pathway downstream of the cAMP/cAMP-dependent protein kinase signal (Fig. 9). Confocal microscopy and quantification of AQP2 signal intensity by image analysis revealed that a synthetic peptide corresponding to the C terminus of the $G_{i3}$ $\alpha$ subunit ($G\alpha_{i3}$ peptide) inhibited the cAMP-induced AQP2 translocation in a concentration-dependent manner, reaching a maximal inhibitory effect at 50–100 $\mu$g/ml. At this concentration, the redistribution of AQP2 appeared to be completely suppressed. Employed at concentrations up to 100 $\mu$g/ml, a peptide corresponding to the C termini of the $\alpha$ subunits of $G_{i1}$ and $G_{i2}$ ($G\alpha_{i1/2}$ peptide) was inactive; a 20–25% inhibition was observed at a concentration of 200 $\mu$g/ml. A peptide with the amino acid composition of the $G\alpha_{i3}$ peptide but with a reversed sequence was inactive even at a high concentration (200 $\mu$g/ml). The latter finding indicates that the inhibitory effects of the $G\alpha_{i1/2}$ and $G\alpha_{i3}$ peptides are specific, *i.e.* are due to functional inhibition of $G_i$ proteins.

The C termini of the $G_i$ $\alpha$ subunits show a very high degree of sequence identity. In fact the $G\alpha_{i1/2}$ and $G\alpha_{i3}$ peptides differ by only two amino acids (see "Experimental Procedures"). It is therefore plausible that the two peptides loose their subtype specificity if employed at a high concentration. Alternatively, several $G_i$ subtypes may in principle be capable of regulating AQP2 trafficking, indicating redundancy with regard to the regulation of a key component controlling the excretion of water. The higher potency of the $G\alpha_{i3}$ peptide compared with that of the $G\alpha_{i1/2}$ peptide suggests that under physiological conditions, $G\alpha_{i3}$ is primarily involved in AQP2 trafficking. In ATP-permeabilized mast cells the $G\alpha_{i3}$ peptide inhibits exocytosis, whereas a peptide (KENLKDCGLF) with 90% identity to a C-terminal portion of the $G_{i2}$ $\alpha$ subunit is less potent (19).

The finding that PTX, an inhibitor of G protein function, also inhibits AQP2 trafficking strongly suggests that PTX-sensitive G proteins stimulate or facilitate insertion of AQP2 into the apical membrane. They may either promote early events (*i.e.* targeting of AQP-bearing vesicles to the apical plasma membrane) or late events (docking/fusion of AQP-bearing vesicles to/with the apical plasma membrane) (Fig. 9). The abundance of $G_i$ proteins on intracellular structures of CD8 cells suggests that G proteins at these locations rather than those associated with the plasma membrane are involved in AQP2 trafficking, although in mast cells the $G_{i3}$ $\alpha$ subunit involved in regulated exocytosis has been located to the plasma membrane (19). During revision of the manuscript, the association of $G_{i3}$ $\alpha$ subunit with secretory vesicles was reported (25). Interestingly, the authors suggest an involvement of $G_{i3}$ in vesicle swelling, a potentially important prerequisite for the fusion of vesicles with the cell plasma membrane. For a proximal kidney tubule cell line (LLC-PK1) an inhibitory role for the $G_{i3}$ $\alpha$ subunit in the constitutive secretion of heparan sulfate proteoglycan has been reported (26). Thus in kidney epithelial cells $G_{i3}$ may have a dual role in vesicular transport, *i.e.* inhibition of constitutive exocytosis and promotion of regulated exocytosis. Alternatively, the $G_{i3}$ $\alpha$ subunit may serve different functions in CD8 and LLC-PK1 cells.

Sands *et al.* (27), by applying the Western blot technique, reported the presence of the $\alpha$ subunits of $G_{q/11}$, $G_{i1}$, $G_{i2}$ and $G_{i3}$ in isolated rat kidney endosomes. Our data are in agreement with theirs regarding the presence of all known $G_i$ $\alpha$ subunits in the rat kidney preparation. In rabbit kidney, however, $G_{i1}$ appears to be expressed at low levels. While Sands *et al.* postulate an inhibitory role of $G_i$ $\alpha$ subunits in translocation of AQP2 to the apical membrane (counteracting the effect of vasopressin), we demonstrate here their involvement in the vasopressin-induced insertion of AQP2 in the apical membrane.

The mechanisms by which G proteins control vesicular transport is not understood (7, 8). Although we have not addressed this problem, the present data provide some hints. G proteins in fractions enriched in AQP2-bearing vesicles are excellent

Downloaded from http://www.jbc.org/ by guest on July 25, 2018

substrates for PTX (Fig. 3), suggesting that they are present as $\alpha\beta\gamma$ heterotrimers. Consistent with this view, both G protein $\alpha$ and $\beta$ subunits were detected in these preparations. In general, the heterotrimeric form of a G protein is required for its interaction with activated plasma membrane receptors, and PTX prevents receptor-mediated but not receptor-independent activation of G proteins (reviewed in Ref. 28). The inhibitory effect of PTX on receptor/G protein coupling and a plethora of other data (reviewed in Ref. 29) show that the C termini of G protein $\alpha$ subunits are important contact sites for receptors. We show here that PTX and peptides corresponding to the C termini of $G_i$ $\alpha$ subunits inhibit AQP2 trafficking. These findings suggest that similar to the well known receptor/G protein interactions, a heterotrimeric G protein is involved in AQP2 trafficking and that the C terminus of its $\alpha$ subunit is required for the interaction with an unknown, possibly upstream, signaling component.

The detection of synaptobrevin 2, Rab3a, and syntaxin 4 in principal cells suggests that these proteins, known to be involved in the $Ca^{2+}$-triggered exocytosis in secretory cells, also participate in the cAMP-triggered fusion of AQP2-bearing vesicles with the apical plasma membrane (6, 30, 31). A role for synaptobrevin 2 in this process is supported by the finding that tetanus toxin, which cleaves synaptobrevin 2, inhibits the homotypic fusion of purified AQP2-bearing vesicles *in vitro* (32). We show here the functional involvement of a PTX-sensitive G protein in cAMP-induced insertion of AQP2 in the apical plasma membrane of principal cells *in vivo*, thereby defining a component required for cAMP-triggered exocytosis in renal epithelial cells. Future studies should lead to the identification of further proteins involved in this process, in particular of those forming the functional link between the cAMP/cAMP-dependent protein kinase signal and vesicle targeting, docking, or fusion.

*Acknowledgments*—We thank Mariano Rocchi and Domenico Pignone (Bari) for valuable advice in image analysis, Michael Beyermann (Berlin) for peptide synthesis, Petra Kronich (Gießen) for excellent technical assistance, and Reinhard Jahn (New Heaven) and John Dixon (Berlin) for critical reading of the manuscript.

REFERENCES

1. Wade, J. B. (1994) *Nephrology* **14,** 322–332
2. Knepper, M., Inoue, T. (1997) *Curr. Opin.Cell Biol.* **9,** 560–564
3. Nielsen, S., Muller, J., and Knepper, M. A. (1993) *Am. J. Physiol.* **265,** F225–F238
4. Nuoffer, C., and Balch, W. E. (1994) *Annu. Rev. Biochem.* **63,** 949–990
5. Novick, P., and Brennwald, P. (1993) *Cell* **75,** 597–601
6. Liebenhoff, U., and Rosenthal, W. (1995) *FEBS Lett.* **365,** 209–213
7. Helms, J. B. (1995) *FEBS Lett.* **369,** 84–88
8. Nürnberg, B., and Ahnert-Hilger, G. (1996) *FEBS Lett.* **389,** 61–65
9. Wollheim, C. B., Lang, J., and Regazzi, R. (1996) *Diabetes Rev.* **4,** 276–297
10. Valenti, G., Frigeri, A., Ronco P. M., D'Ettorre, C., and Svelto M. (1996) *J. Biol. Chem.* **271,** 24365–24370; Correction (1997) *J. Biol. Chem.* **272,** 26794
11. Vandewalle, A., Lelongt, B., Géniteau-Legendre, M., Baudouin, B., Antoine, M., Estrade, S., Châtelet, F., Verroust, P., Cassingéna, R., and Ronco, P. (1989) *J. Cell. Physiol.* **141,** 203–221
12. Deleted in proof
13. Farinas, J., Simanek, V., and Verkman, A. S. (1995) *Biophys. J.* **68,** 1613–1620
14. Leopoldt, D., Harteneck, C., and Nürnberg, B. (1997) *Naunyn-Schmiedebergs Arch. Pharmakol.* **356,** 216–224, and references therein
15. Schmidt, A., Hescheler, J., Offermanns, S., Spicher, K., Hinsch, K-D., Klinz, F-J., Codina, J., Birnbaumer, L., Gausepohl, H., Frank, R., Schultz, G., and Rosenthal, W. (1991) *J. Biol. Chem.* **266,** 18025–18033
16. Benedetti, P. A., Evangelista, V., Guidarini, D., and Vestri, S. (1995a) *Zool. Studies* **34,** Suppl. 1, 186–188
17. Benedetti, P. A., Evangelista, V., Guidarini, D., and Vestri, S. (1995b) *SPIE—The International Society for Optical Engineering* **2412,** 56–62
18. Ahnert-Hilger, G., Mach, W., Fohr, K. J., and Gratzl, M. (1989) *Methods Cell Biol.* **31,** 63–90C
19. Aridor, M., Rajmilevich, G., Beaven, M. A., and Sagi-Eisenberg, R. (1993) *Science* **262,** 1569–1572, and references therein
20. Sabolic, I., Wuarin, F., Shi, L-B. Verkman, A. S., Ausiello, D. A., Gluck, S., and Brown, D. (1992) *J. Cell Biol.* **119,** 111–122
21. Rudolph, U., Koesling, D., Hinsch, K.-D., Seifert, R., Bigalke, M., Schultz, G., and Rosenthal, W. (1989) *Mol. Cell. Endocrinol.* **63,** 143–153
22. Ercolani, L., Stow, J. L., Boyle, J. F., Holtzman, E. J., Lin, H., Grove, J. R., and Ausiello, D. A. (1990) *Proc. Natl. Acad. Sci. U. S. A.* **87,** 4635–4639
23. Katsura, T., Gustafson, C. E., Ausiello, D. A., and Brown, D. (1997) *Am. J. Physiol.* **272,** F816–F822
24. Fushimi, K., Sasaki, S., Marumo, F. (1997) *J. Biol. Chem.* **272,** 14800–14804
25. Jena, B. P., Schneider, S. W., Geibel, J., Webster, P., Oberleithner, H., and Sritharan, K. C. (1997) *Proc. Natl. Acad. Sci. U. S. A.* **94,** 13317–13322
26. Stow, J. L., de Almeida, J. B., Narula, N., Holtzman, E. J., Ercolani, L., and Ausiello, D. A. (1991) *J. Cell Biol.* **114,** 1113–1124
27. Sands, J. M., Naruse, M., Baum, M., Hebert, S. C., Brown, E. M., and Harris, H. W. (1997) *J. Clin. Invest.* **99,** 1399–1405
28. Birnbaumer, L., Abramowitz, J., and Brown, A. M. (1990) *Biochim. Biophys. Acta* **1031,** 163–224
29. Lambright, D. G., Sondek, J., Bohm, A., Skiba, N. P., Hamm H. E., and Sigler, P. B. (1996) *Nature* **379,** 311–319
30. Nielsen, S., Chou, C. L., Marples, D., Christensen, E. I., Kishore, B. K., and Knepper, M. A. (1995) *Proc. Natl. Acad. Sci. U. S. A.* **92,** 1013–1017
31. Mandon, B., Chou, C. L., Nielsen, S., and Knepper, M. A. (1996) *J. Clin. Invest.* **98,** 906–913
32. Jo, I., Harris, H. W., Amendt-Raduege, A. M., Majewski, R. R., and Hammond, T. G. (1995) *Proc. Natl. Acad. Sci. U. S. A.* **92,** 1976–1880

Downloaded from http://www.jbc.org/ by guest on July 25, 2018

# A Heterotrimeric G Protein of the $G_i$ Family Is Required for cAMP-triggered Trafficking of Aquaporin 2 in Kidney Epithelial Cells

Giovanna Valenti, Giuseppe Procino, Ursula Liebenhoff, Antonio Frigeri, Pio Alberto Benedetti, Gudrun Ahnert-Hilger, Bernd Nürnberg, Maria Svelto and Walter Rosenthal

*J. Biol. Chem. 1998, 273:22627-22634.*
*doi: 10.1074/jbc.273.35.22627*

---

Access the most updated version of this article at http://www.jbc.org/content/273/35/22627

Alerts:
- When this article is cited
- When a correction for this article is posted

Click here to choose from all of JBC's e-mail alerts

This article cites 30 references, 9 of which can be accessed free at
http://www.jbc.org/content/273/35/22627.full.html#ref-list-1

Downloaded from http://www.jbc.org/ by guest on July 25, 2018